Clinical Neurophysiology 131 (2020) 2713–2715

Contents lists available at ScienceDirect

Clinical Neurophysiology

journal homepage: www.elsevier.com/locate/clinph

Letter to the Editor

MEG and high-density EEG resting-state networks mapping in children

Resting-state networks (RSNs) are mostly studied using functional magnetic resonance imaging (fMRI) (Zhang and Raichle, 2010). Still, fMRI relies on the hemodynamic response, which is an indirect measure of brain activity that can be modified by age or brain disorders. Electrophysiological techniques such as magnetoencephalography (MEG) or electroencephalography (EEG) overcome this limitation by providing direct measures of brain activity. Electrophysiological RSNs emerge from large-scale correlation patterns in the slow fluctuations of MEG/EEG band-limited power envelope (Coquelet et al., 2020). In adults, when using seed-based connectivity mapping, MEG provides similar spatial architecture than high-density EEG (hdEEG) for low-level RSNs (i.e., sensorimotor (SM1), auditory (A1), visual (V1) RSNs) but differences occur for high-level RSNs (i.e., default-mode network (DMN), fronto-parietal network (FPN)) (Coquelet et al., 2020). Whether these results extend to children remains unsettled. Such data would be of high interest considering the wide availability of EEG and its key interest for lifespan or clinical studies.

This seed-based resting-state functional connectivity (rsFC) study compared the spatial signature of five major MEG and hdEEG RSNs in typically developing children based on simultaneous MEG/hdEEG recordings of resting brain activity. We expected (i) that both modalities would yield similar low-level RSNs but discrepancies for high-level RSNs, and (ii) to find established low-level RSNs and rather immature high-level RSNs due to developmental effects.

Resting-state brain activity of 36 children (14 girls, 3 left-handed, mean age ± SD: 9.91 ± 1.37 years, age range: 7–11 years, no neurological/psychiatric or cognitive disorder) was recorded (2 sessions of 5 min) using simultaneous 306-channel MEG (Triux, MEGIN, Finland) and MEG-compatible 256-channel scalp hdEEG (Hydrocel sensor nets, EGI Philips, USA). Subjects were asked to sit still, with eyes opened, and to gaze at a picture of their favorite cartoon. High-resolution 3D T1-weighted brain MRI was also obtained in each participant (1.5 Tesla MRI, Intera, Philips, Netherlands, for 20 subjects, or hybrid 3 T PET-MRI scanner, Signa, General Electrics Healthcare, Wisconsin, USA, for 16 subjects). Twelve children were excluded due to excessive movement artifacts. Written informed consent was obtained from all participants and their legal representative, after approval by institutional Ethics Committee (Reference: P2018/179).

In a nutshell, signal space separation was applied offline to MEG data to subtract environmental magnetic noise and correct for head movements. Bad EEG channels were detected and reconstructed with an *in-house* automated pipeline. Ocular, cardiac, and remaining system artifacts were further eliminated using an independent component analysis of the band-passed (1–40 Hz) MEG and hdEEG data separately. Artefactual components were identified and regressed out of the full-rank data. hdEEG data were restricted to 172 scalp electrodes and then re-referenced to their average.

Forward models were computed based on participants' segmented MRI, co-registered to MEG/hdEEG coordinate systems. A volumetric, regular 5-mm source grid was built and non-linearly deformed onto each participant's MRI. Three orthogonal current dipoles were then placed at each grid point. MEG forward modeling was performed on this source space using a one-layer boundary element method (BEM). For hdEEG, two different forward models were considered: a three-layer BEM (BEM_3; conductivity values: σ_{brain} = 0.33/Ωm, σ_{skull} = 0.006/Ωm, and σ_{scalp} = 0.33/Ωm) and a five-compartment finite element model (FEM_5; conductivity values: $\sigma_{white\ matter}$ = 0.14/Ωm, $\sigma_{gray\ matter}$ = 0.33/Ωm, $\sigma_{cerebrospinal\ fluid}$ = 1.79/Ωm, σ_{skull} = 0.01/Ωm, σ_{scalp} = 0.43/Ωm).

Seed-based MEG/hdEEG rsFC maps of five major RSNs were computed in their preferential frequency bands as in (Wens et al., 2014; Coquelet et al., 2020): SM1, seed MNI coordinates: [42,–26,54] mm, 13–30 Hz; A1, [54,–22,10], 13–30 Hz; V1, [20,–86,18], 8–12 Hz; DMN, [–2,51,2], 8–12 Hz; FPN, [34,20,44], 13–30 Hz. Minimum norm estimation was applied to reconstruct sources of band-limited activity and spatial leakage was corrected using signal orthogonalization. The individual rsFC maps were then obtained as envelope correlation maps between the seed and orthogonalized source time courses (see Wens et al., 2014; Coquelet et al., 2020 for illustration) and finally group averaged. Complete details regarding preprocessing and data analysis methods along with relevant references are detailed in Coquelet et al. (2020).

Fig. 1 depicts the resulting seed-based MEG/hdEEG rsFC maps obtained in children.

MEG and hdEEG (BEM_3 and FEM_5) allowed for the proper identification of the typical inter-hemispheric rsFC for A1 and V1 low-level RSNs. For the SM1 RSN, only MEG disclosed a clear local correlation maximum at the SM1 cortex contralateral to the seed, while hdEEG (BEM_3 and FEM_5) rsFC maps were dominated by intra-hemispheric rsFC.

For high-level RSNs (i.e., DMN and FPN), both MEG and hdEEG analyses did not reveal the typical RSNs spatial architecture reported in the previous literature (Coquelet et al., 2020). For the DMN, no rsFC was observed from the mesial prefrontal seed either with the posterior midline cortices (i.e., precuneus and posterior cingulate cortex), nor with bilateral temporo-parietal junctions that are major nodes of the electrophysiological DMN. For the FPN, rsFC with the right superior frontal seed was either dominated by intra- and inter-hemispheric prefrontal correlation (MEG and hdEEG-BEM_3), or by intra-hemispheric prefrontal and temporal correlation (hdEEG-FEM_5).

https://doi.org/10.1016/j.clinph.2020.09.003

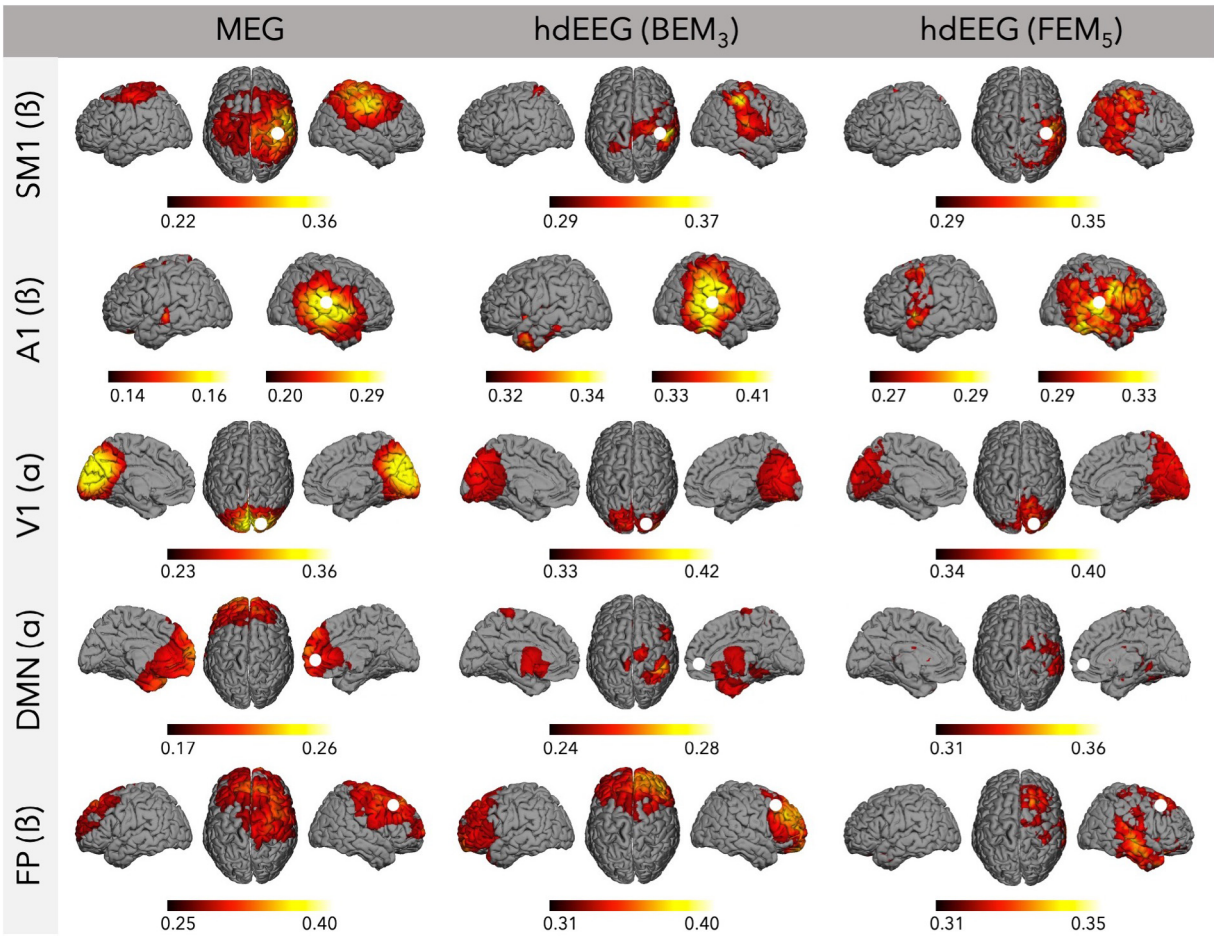

Fig. 1. Spatial maps of the five RSNs of interest using MEG (first column), hdEEG BEM_3 (second column) and hdEEG FEM_5 (third column): primary Sensorimotor (SM1; seed MNI coordinates: [42,–26,54] mm; β band), Auditory (A1; [54,–22,10] mm; β), Visual (V1; [20,–86,18] mm; α), Default-Mode Network (DMN; [–2,51,2] mm; α) and Fronto-Parietal (FP; [34,20,44] mm; β). Thresholds of RSN maps are calculated from mean + 1SD (min) to mean + 2.5SD (max).

Thus, MEG and hdEEG provide similar inter-hemispheric spatial architecture for low-level RSNs in children, except for SM1 RSN that is best captured by MEG. For high-level RSNs, the absence of typical antero-posterior electrophysiological rsFC between nodes of the considered RSNs is probably related to developmental effects. Indeed, this finding is in line with the early maturation of motor and sensory networks, and the ongoing maturation of high-order cognitive networks during adolescence (Grayson and Fair, 2017; Briley et al., 2018).

EEG signals were recorded with MEG-compatible passive EEG electrodes. Such electrodes are increasingly used in pediatric settings as they allow recordings of hdEEG (i.e., 256 electrodes) with drastic reduction of the preparation time (about 15 min). Still, passive EEG systems provide lower signal to noise ratio than active systems, wherein signals are amplified on the scalp to minimize interferences picked up by the cables. So, further studies are needed to generalize our results to other types of EEG systems. This aspect might also have contributed to the lower ability of hdEEG to uncover the SM1 RSN.

Declaration of Competing Interest

The authors declare that they have no known competing financial interests or personal relationships that could have appeared to influence the work reported in this paper.

Acknowledgements

The MEG / hdEEG project at the CUB Hôpital Erasme is financially supported by "Fondation ROGER DE SPOELBERCH". Dorine Van Dyck is supported by "The Belgian Kids' Fund for Pediatric Research". Nicolas Coquelet has been supported by the ARCC and is supported by the Fonds Erasme (Research Convention "Les Voies du Savoir", Brussels, Belgium). Xavier De Tiège is Postdoctorate Clinical Master Specialist at the FRS-FNRS. The authors would like to thank warmly all the children and their parents for their participation.

References

Briley PM, Liddle EB, Groom MJ, Smith HJF, Morris PG, Colclough GL, et al. Development of human electrophysiological brain networks. J Neurophysiol 2018;120:3122–30.
Coquelet N, De Tiège X, Destoky F, Roshchupkina L, Bourguignon M, Goldman S, et al. Comparing MEG and high-density EEG for intrinsic functional connectivity mapping. Neuroimage 2020;210. 116556.
Grayson DS, Fair DA. Development of large-scale functional networks from birth to adulthood: A guide to the neuroimaging literature. Neuroimage 2017;160:15–31.
Wens V, Mary A, Bourguignon M, Goldman S, Marty B, Op de Beeck M, et al. About the electrophysiological basis of resting state networks. Clin Neurophysiol 2014;125:1711–3.
Zhang D, Raichle ME. Disease and the brain's dark energy. Nat Rev Neurol 2010;6:15–28.

Dorine Van Dyck *,[1]
Laboratoire de Cartographie fonctionnelle du Cerveau, UNI – ULB, Neurosciences Institute, Université libre de Bruxelles (ULB), Brussels, Belgium
Department of Neurology, Hôpital Universitaire des Enfants Reine Fabiola (HUDERF), Université libre de Bruxelles (ULB), Brussels, Belgium
* Corresponding author at: Laboratoire de Cartographie fonctionnelle du Cerveau, ULB Neuroscience Institute, Université libre de Bruxelles (ULB), 808 Lennik Street, 1070 Brussels, Belgium
E-mail address: dorine.van.dyck@ulb.be

Nicolas Coquelet [1]
Laboratoire de Cartographie fonctionnelle du Cerveau, UNI – ULB, Neurosciences Institute, Université libre de Bruxelles (ULB), Brussels, Belgium

Nicolas Deconinck
Department of Neurology, Hôpital Universitaire des Enfants Reine Fabiola (HUDERF), Université libre de Bruxelles (ULB), Brussels, Belgium

Alec Aeby
Department of Neurology, Hôpital Universitaire des Enfants Reine Fabiola (HUDERF), Université libre de Bruxelles (ULB), Brussels, Belgium

Simon Baijot
Department of Neurology, Hôpital Universitaire des Enfants Reine Fabiola (HUDERF), Université libre de Bruxelles (ULB), Brussels, Belgium

Serge Goldman
Department of Functional Neuroimaging, Service of Nuclear Medicine, CUB Hôpital Erasme, Université libre de Bruxelles, Brussels, Belgium

Charline Urbain
Laboratoire de Cartographie fonctionnelle du Cerveau, UNI – ULB, Neurosciences Institute, Université libre de Bruxelles (ULB), Brussels, Belgium
UR2NF, Neuropsychology and Functional Neuroimaging Research Group at CRCN, Center for Research in Cognition and Neurosciences and ULB Neurosciences Institute (UNI), ULB, Brussels, Belgium

Nicola Trotta
Laboratoire de Cartographie fonctionnelle du Cerveau, UNI – ULB, Neurosciences Institute, Université libre de Bruxelles (ULB), Brussels, Belgium
Department of Functional Neuroimaging, Service of Nuclear Medicine, CUB Hôpital Erasme, Université libre de Bruxelles, Brussels, Belgium

Vincent Wens
Laboratoire de Cartographie fonctionnelle du Cerveau, UNI – ULB, Neurosciences Institute, Université libre de Bruxelles (ULB), Brussels, Belgium
Department of Functional Neuroimaging, Service of Nuclear Medicine, CUB Hôpital Erasme, Université libre de Bruxelles, Brussels, Belgium

Xavier De Tiège
Laboratoire de Cartographie fonctionnelle du Cerveau, UNI – ULB, Neurosciences Institute, Université libre de Bruxelles (ULB), Brussels, Belgium
Department of Functional Neuroimaging, Service of Nuclear Medicine, CUB Hôpital Erasme, Université libre de Bruxelles, Brussels, Belgium

Accepted 7 September 2020

Available online 23 September 2020

[1] Contributed equally.